Annual Review of Physiology

Calcium Regulation of Mitochondrial Metabolism

Carmen A. Mannella,[1,2] Pawel Swietach,[3] and Liron Boyman[3]

[1]Center for Biomedical Engineering and Technology, University of Maryland School of Medicine, Baltimore, Maryland, USA

[2]Department of Physiology, Pharmacology and Drug Discovery, University of Maryland School of Medicine, Baltimore, Maryland, USA

[3]Department of Physiology, Anatomy and Genetics, University of Oxford, Oxford, United Kingdom; email: liron.boyman@dpag.ox.ac.uk

Annu. Rev. Physiol. 2026. 88:17.1–17.23

The *Annual Review of Physiology* is online at physiol.annualreviews.org

https://doi.org/10.1146/annurev-physiol-052424-082740

Keywords

mitochondria, energy metabolism, ATP, calcium, mitochondrial calcium signaling, mitochondrial calcium uniporter

Abstract

Mitochondrial ATP production dynamically adapts to cellular energy demands, with calcium (Ca^{2+}) playing a crucial regulatory role. In this review, we critically evaluate the evidence for intramitochondrial Ca^{2+} ($[Ca^{2+}]_m$) sensitivity in key energy metabolic pathways, highlighting the $[Ca^{2+}]_m$ dependence of specific mitochondrial systems. We also address the metabolic consequences of $[Ca^{2+}]_m$-sensitive ATP production, particularly its effects on the utilization of specific macronutrients that fuel ATP production. Next, we discuss the primary Ca^{2+} entry pathway into the matrix, the mitochondrial Ca^{2+} uniporter (MCU), its macromolecular complex structure (MCUcx), and allosteric regulation by Ca^{2+}. Key to this regulation are specific auxiliary subunits, along with the influence of mitochondrial inner membrane architecture. While the Ca^{2+} signaling plays an important role, it does not fully explain the scope for regulating ATP production. Emerging evidence suggests that additional signaling systems operating alongside the Ca^{2+} signaling contribute to the control of mitochondrial ATP production, a topic requiring further investigation.

1. INTRODUCTION

Cytosolic calcium (Ca^{2+}) signaling is a highly adaptable mechanism regulating diverse cellular processes across various eukaryotic cell types (1, 2). Its direct influence extends to controlling muscle contraction, neurotransmission, and numerous other fundamental functions. Importantly, beyond these direct effects, Ca^{2+} signaling also modulates parallel processes that provide essential support. One such vital parallel signaling pathway is the regulation of ATP production within mitochondria, ensuring that the energy consumed by cellular processes is replenished.

Since its initial identification in the 1970s (3), our understanding of this unique and highly compartmentalized mitochondrial Ca^{2+} signaling pathway has expanded tremendously. With the advent of new research tools and technologies, both the biophysical and molecular understanding of the major transport systems facilitating the movement of Ca^{2+} across the inner mitochondrial membrane (IMM) have become clearer. However, some systems remain uncertain and are the focus of ongoing investigations. Similarly, the enzyme processes and protein systems targeted by mitochondrial Ca^{2+} regulation continue to be updated. It has also become increasingly apparent that mitochondrial Ca^{2+} signaling is highly specialized, varying significantly between tissues and further altering during disease development.

In this review, we examine the literature exploring how mitochondrial matrix Ca^{2+} ($[Ca^{2+}]_m$) regulates ATP production. We also provide an updated review of the molecular and quantitative aspects of mitochondrial Ca^{2+} signaling. Additionally, we present a detailed discussion of the current understanding of the primary pathway for Ca entry into the mitochondrial matrix, the mitochondrial Ca^{2+} uniporter holo-complex (MCUcx). Finally, we highlight a novel signaling system operating alongside the mitochondrial Ca^{2+} signaling system, which broadens its regulatory range.

2. PHYSIOLOGICAL REGULATION OF MITOCHONDRIAL ATP PRODUCTION

In tissues characterized by high energy demand, notably the liver, kidneys, heart, and brain, mitochondria serve as the primary source of cellular ATP. It is thus not surprising that mitochondria make up 22% of the cellular volume in the kidney and liver (4–6) and at least 30% in heart muscle cells (7). The dynamic range of mitochondrial ATP production, inferred from tissue oxygen consumption under baseline and stimulated conditions, varies widely among tissues, reflecting regulatory scope (**Figure 1*a*,*b***). In the liver and kidney, oxygen consumption rises only modestly (up to 25%) above baseline levels (8–15). On the other hand, the heart—especially under elevated adrenergic tone and circulatory demand—can undergo a substantial increase in oxygen consumption, with estimates in the range 2.5- to fivefold (16–25). Even more pronounced increases have been reported in skeletal muscle, where oxygen consumption can rise by 6 to 17 times above baseline (26–29).

The scope for increasing mitochondrial ATP production depends, in part, on blood-borne delivery of oxygen and carbon-based energy sources. This extrinsic regulation highlights the importance of coupling metabolic demand with blood perfusion, operated through various feedback mechanisms between tissues and its vascular smooth muscle cells (30). Regulatory mechanisms intrinsic to the mitochondrion also play a role in managing ATP production, many of which have long been hypothesized to be sensitive to calcium ions (Ca^{2+}), with evidence dating back to the 1970s (3). This early evidence was strengthened by subsequent findings, giving rise to the view that the intramitochondrial calcium concentration acts as a signal to regulate mitochondrial metabolism. Herein, we critically review the evidence and discuss the implications of this oversight mechanism in the heart and nonexcitable tissues.

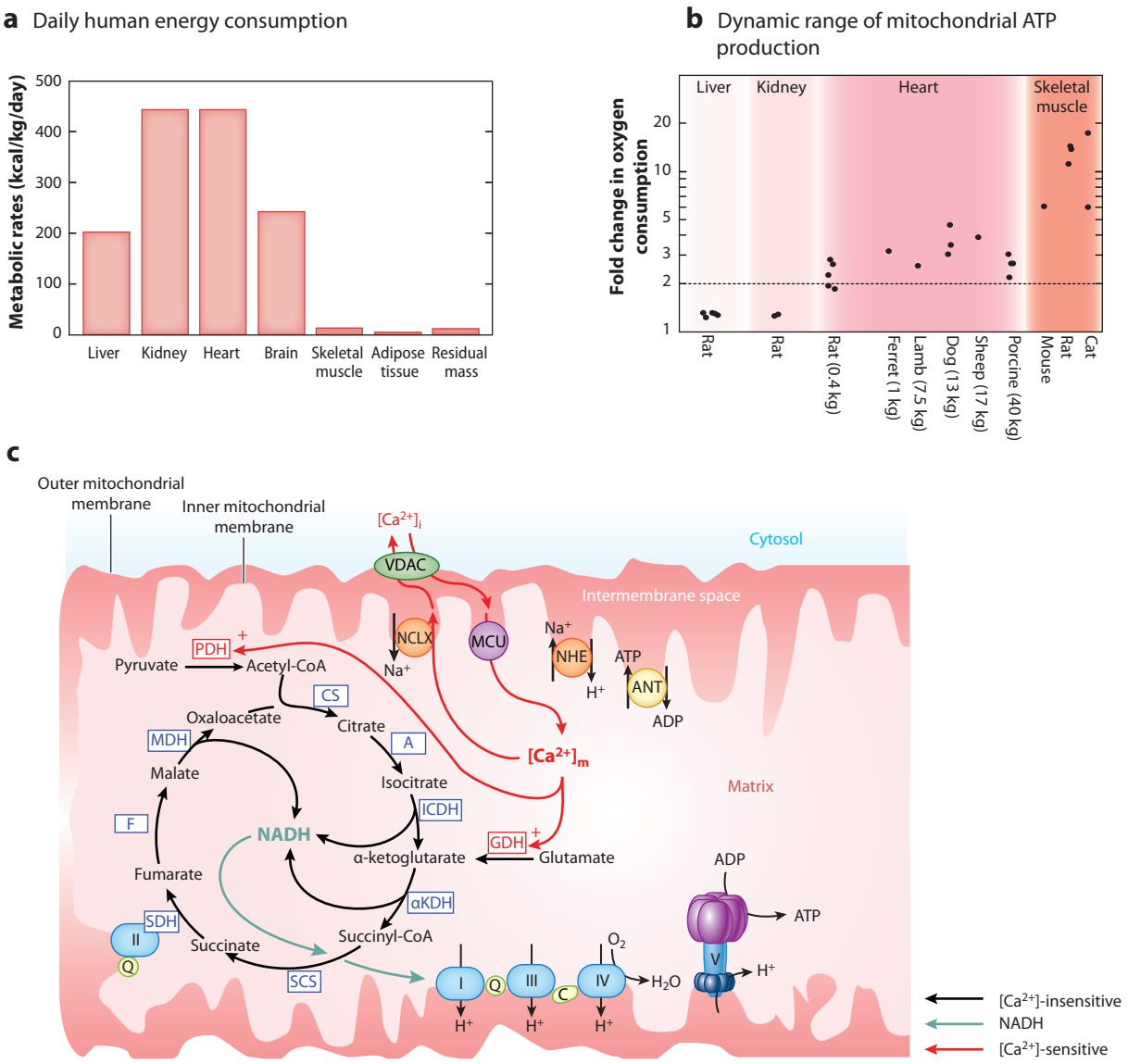

Figure 1

Energy consumption, its dynamic range, and the physiological regulation of ATP production by mitochondrial calcium. (*a*) Daily metabolic rates of major organs and tissues. Shown values are from human subjects. Data from Reference 31. (*b*) Fold changes in oxygen consumption rates of different tissues in different species. Each data point shows the fold change in oxygen consumption determined by distinct studies performed in liver (8–13), kidney (14, 15), heart (16–25), and skeletal muscle (26–29). All shown measurements were carried out with healthy tissues of wild-type animals under similar, physiologically relevant basal and strenuous activities. The indicated weight (in kilograms) is the total body weight. (*c*) Schematic diagram of the interaction of matrix Ca^{2+} ($[Ca^{2+}]_m$) with processes and systems involved in oxidative phosphorylation. The complexes of oxidative phosphorylation are labeled I–V. The red arrows pointing from Ca^{2+} to the various interaction sites suggest a direct or indirect modulation of enzymatic activity. Abbreviations: A, aconitase; αKDH, α-ketoglutarate dehydrogenase; ANT, adenine nucleotide translocase; C, cytochrome C; CS, citrate synthase; F, fumarase; ICDH, isocitrate dehydrogenase; MDH, malate dehydrogenase; MCU, mitochondrial calcium uniporter; NCLX, the mitochondrial sodium calcium exchanger; NHE, the mitochondrial proton sodium exchanger; PDH, pyruvate dehydrogenase; Q, coenzyme Q; SCS, succinyl-CoA synthetase; SDH, succinate dehydrogenase (also complex II); VDAC, voltage-dependent anion-selective channel.

3. CALCIUM REGULATION OF INTRA-MITOCHONDRIAL ENERGY METABOLISM

The Krebs cycle dehydrogenase enzymes, along with the dehydrogenases that feed intermediates into the cycle, generally catalyze the reduction of NAD^+ to NADH while releasing CO_2. This NADH energizes the electron transport chain that sets up the electrochemical $[H^+]$ gradient across the IMM, which in turn, powers ATP synthase. The regulation of these matrix-localized dehydrogenases by Ca^{2+} establishes a direct line of communication between cellular Ca^{2+} signals and the control of energy metabolism. This potential role of mitochondrial Ca^{2+} signals was first identified in research conducted more than 50 years ago (3) and remains widely accepted today, although the understanding of its molecular underpinnings have evolved considerably since.

3.1. Biochemical Studies

In 1969, Reed and colleagues demonstrated that the pyruvate dehydrogenase (PDH) complex in mammalian tissues is regulated by reversible phosphorylation (32). This phosphorylation is mediated by a kinase tightly bound to the complex, leading to an almost complete loss of PDH activity. Reactivation occurs through a magnesium-activated phosphatase (32). These discoveries paved the way for Denton and colleagues in 1972 to examine the properties of this enzyme in greater detail (3). By using EGTA buffers, it was revealed that the phosphatase in various mammalian tissues is activated by Ca^{2+}, with an estimated $K_{0.5}$ value close to 1 μM (3). Because PDH links glycolysis to the Krebs cycle, this report seeded the view that Ca^{2+} regulates intramitochondrial metabolism.

In the late 1970s, Denton, McCormack, and their colleagues at the University of Bristol investigated the Ca^{2+} sensitivity of various mitochondrial dehydrogenases besides PDH (33–35). At that time, none of these dehydrogenases were known to be regulated through post-translational modifications. As a result, instead of examining possible Ca^{2+} sensitivity of kinases/phosphatases, they focused on assessing how Ca^{2+} influenced the reactions catalyzed by specific dehydrogenases present in extracts of mammalian mitochondria. To infer dehydrogenase activity, changes in absorbance tracked the production of NAD(P)H in response to specific substrates and measured over a range of $[Ca^{2+}]$. In their screen, two enzymatic reactions were found to be Ca^{2+} sensitive: NADH production evoked by either isocitrate (33, 34) or α-ketoglutarate (34, 35). These results led to the conclusion that isocitrate dehydrogenase (ICDH) and α-ketoglutarate dehydrogenase (αKDH), along with PDH, are the only Ca^{2+}-sensitive dehydrogenases in the matrix. Furthermore, the enzymes' $K_{0.5}$ values for Ca^{2+} of ∼1 μM were interpreted to signify physiological significance. However, subsequent studies, summarized in **Table 1**, revised this early interpretation.

In the mid- to late 1980s, Denton and McCormack, now collaborating with other colleagues, reevaluated their earlier conclusions using newly available research tools that offered improved precision and specificity (36, 37). They reexamined the properties of ICDH in rat heart mitochondrial extracts and in permeabilized mitochondria. In both cases, considerably higher $K_{0.5}$ values for Ca^{2+} were obtained (∼10 μM). The discrepancy with early estimates was attributed to improved tools to measure and control free $[Ca^{2+}]$ and the presence of physiological $[K^+]$ (36, 37). Critically, these subsequent studies cast doubt on the physiological relevance of ICDH regulation by Ca^{2+}, which now appeared to occur well above the physiological range for mitochondrial $[Ca^{2+}]$. Another aspect of the research that was revisited was the characterization of αKDH. They aimed to examine the possibility that Ca^{2+} might be impacting an upstream step in this metabolic pathway, possibly involving glutamate dehydrogenase (GDH), which converts glutamate to α-ketoglutarate. The resulting findings supported this possibility. In particular,

Table 1 Biochemical investigations of the Ca^{2+} sensitivity of matrix-localized dehydrogenases

Enzyme	Study	Preparation	Assay	$[Ca^{2+}]$ $K_{0.5}$ (μM)	Ca^{2+} measurement	Mechanism of action
PDH	3	Pyruvate dehydrogenase and pyruvate dehydrogenase phosphate extracted from a pig heart mitochondrial fraction	Release of $[^{32}P]P_i$ from pig heart PDH $[^{32}P]$phosphate	1	Computational buffering tables (54)	PDH phosphatase activation
	38	Extracts of rat liver mitochondria	Assay of PDHP-phosphatase activity	1.41	Computational buffering tables (54)	PDH phosphatase activation
ICDH	33	Extracts of rat mitochondria from heart, liver, kidney, brown adipose tissue and white adipose tissue	NADH production (absorption)	1.2–1.67	Computational buffering tables (54)	ND
	55	Partially purified fraction from extracts of bovine heart	NADH production (absorption)	0.6–0.65	Atomic absorption spectrometry	ND
	34	Mitochondria extracts from hearts of rat, pigeon, trout, and frog, and from human heart tissue	NADH production (absorption)	1.1–1.2	Computational buffering tables (54)	ND
	38	Partially purified fraction from extracts of rat liver mitochondria	NADH production (absorption), $^{14}CO_2$ production	0.91	Computational buffering tables (54)	ND
	36	Toluene-permeabilized rat heart mitochondria and extracts of permeabilized rat heart mitochondria	NADH production (absorption)	5.5–43	Arsenazo III	ND
	37	Partially purified fraction from extracts of pig heart	NADH production (absorption)	4.7–70	Computational buffering tables (54)	ND

(*Continued*)

Table 1 (*Continued*)

Enzyme	Study	Preparation	Assay	$[Ca^{2+}]$ $K_{0.5}$ (μM)	Ca^{2+} measurement	Mechanism of action
αKDH	35	Mitochondrial extracts from brown adipose tissue, hearts Fractionation of KDH complex from pig heart	NADH production (absorption)	1.2	Computational buffering tables (54)	ND
	34	Extracts form rat heart mitochondria, and human heart tissue Mitochondria from hearts of pigeon, trout, and frog	NADH production (absorption)	0.6–1.1	Computational buffering tables (54)	ND
	38	Extracts of rat liver mitochondria	NADH production (absorption), $^{14}CO_2$ production	0.4–1.22	Computational buffering tables (54)	ND
	36	Toluene-permeabilized rat heart mitochondria and extracts of permeabilized rat heart mitochondria	NADH production (absorption)	0.19–0.4	Arsenazo III	ND
GDH	38	Extracts of rat liver mitochondria	NADH production (absorption), $^{14}CO_2$ production	0.4–1.22	Computational buffering tables (54)	ND

Abbreviations: αKDH, α-ketoglutarate dehydrogenase; GDH, glutamate dehydrogenase; ICDH, NAD^+-linked isocitrate dehydrogenase; NADH, reduced nicotinamide adenine dinucleotide; ND, no data; PDH, pyruvate dehydrogenase; PDHP, pyruvate dehydrogenase phosphatase.

under the conditions of their experiments with mitochondria (38), Ca^{2+} enhanced the rate at which radiolabeled CO_2 ($^{14}CO_2$) was produced from radiolabeled glutamate ([1–^{14}C]glutamate).

In a series of subsequent reviews spanning from the 1990s (39, 40) to 2009 (41), Denton and McCormack, along with their colleagues, still maintained the position that ICDH and αKDH are sensitive to Ca^{2+}. However, they complemented this stance with a comprehensive and critical discussion of their research in light of emergent limitations. Over time, unlike the case for PDH, the support for Ca^{2+} sensitivity of ICDH and αKDH waned due to the lack of a compelling mechanism. No Ca^{2+}-dependent post-translational modifications have been identified, nor have any putative EF-hand motifs or other canonical Ca^{2+} binding sites been found within these enzymatic macrocomplexes.

3.2. Physiological Scrutiny

In 2019, Wescott et al. (42) revisited this issue using newer tools and technologies that, compared with those previously available, significantly improved their ability to manipulate and observe mitochondrial processes with spatiotemporal precision. They measured time-resolved ATP production by intact functional cardiac mitochondria in a physiologically relevant context, while directly measuring $[Ca^{2+}]_m$ with calibrated fluorescent indicators. These experiments were designed to identify the sites of Ca^{2+} regulation by comparing the $[Ca^{2+}]_m$ sensitivity of ATP production powered by diverse metabolic substrates. They examined different carbon sources, such as carbohydrates and amino acids that are metabolized through the Krebs cycle. They also examined lipids, which undergo catabolic steps in the mitochondrial matrix and enter the Krebs cycle after β-oxidation as two-carbon acetyl-CoA or four-carbon succinyl-CoA. The experiments identified specific carbon substrates that enable $[Ca^{2+}]_m$-sensitive ATP production and others that do not. The finding that ATP production powered by lipids is not sensitive to regulation by $[Ca^{2+}]_m$ was unexpected based on prior literature. As the end products of β-oxidation of lipids feed directly into the Krebs cycle, this outcome meant that $[Ca^{2+}]_m$ does not significantly affect enzymatic steps within the Krebs cycle itself, including those catalyzed by ICDH and αKDH. In sharp contrast, other findings showed that the entry of glutamate and pyruvate into the Krebs cycle is regulated by $[Ca^{2+}]_m$, and it is through this regulation that increasing $[Ca^{2+}]_m$ augments ATP production. This constituted direct evidence that $[Ca^{2+}]_m$ regulates ATP production by modulation of PDH and GDH activity, and not through any effects on Krebs cycle dehydrogenases, nor on ATP synthase (complex V) or the electron transport chain complexes II, III or IV, which also had been implicated in previous studies as possible sites at which elevated $[Ca^{2+}]_m$ stimulated ATP production (43).

Glutamate and pyruvate are the breakdown products of proteins and carbohydrates. These findings by Wescott et al. (42) thus identify $[Ca^{2+}]_m$ as a key regulator of mitochondrial utilization of proteins and carbohydrates, but not that of lipids. Further studies using genetic mouse models aligned with this conclusion and revealed the broader metabolic and physiological implications. In particular, mouse models were employed in which the MCU was genetically deleted (44–46). As a result, the ability of Ca^{2+} to enter the mitochondrial matrix and regulate its metabolism was largely attenuated. These mice displayed broad transcriptional adaptation that occurs in response to life without a functional cardiac MCU (44). Importantly, the adaptations that accompany genetic deletion of MCU include changes of mitochondrial fuel selection, with a shift toward mitochondrial fatty acid metabolism in skeletal muscle (45), as well as augmentation of cardiac fatty acid oxidation as compensatory source of high-energy to sustain ATP production (46). These findings further support the suggested role of mitochondrial Ca^{2+} influx as the signal that stimulates pyruvate-fueled ATP production by mitochondria (3, 42). Consequently, in the absence of functional MCU channels, other carbon sources are consumed at higher rates as an adaptive mechanism.

There is no question that further quantitative investigations, under a range of physiological conditions, are necessary to more comprehensively characterize the full spectrum of Ca^{2+} sensitivity in mitochondrial ATP production. Moreover, mitochondrial Ca^{2+} sensitivity is likely to exhibit tissue-specific characteristics, because energy consumption and daily metabolic rates differ significantly across major organs and tissues, as illustrated in **Figure 1**. The mitochondria in different tissues both support and respond to different cellular metabolic pathways and so can access a variety of respiratory fuels under different conditions.

3.3. Sites of Calcium Regulation Outside the Mitochondrial Matrix

The possibility that Ca^{2+}does not need to enter the mitochondrial matrix to regulate energy metabolism has been examined in several studies. Ca^{2+} likely enters mitochondria primarily through the numerous large voltage-dependent anion-selective channel (VDAC) pores in the outer mitochondrial membrane (OMM) and has been shown to influence the permeability properties of VDAC as well as its interactions with partner proteins (reviewed in 47; also see Section 3.2). However, there is as yet no evidence that the effects of Ca^{2+} at the OMM modulate ATP production under physiological conditions. Likewise, identifying sites of Ca^{2+} regulation of ATP production within the mitochondrial intermembrane space (IMS) has proven to be elusive. Indeed, stimulation of mitochondrial metabolism by increasing extramitochondrial [Ca^{2+}] is generally abolished by either Ruthenium Red or Ru360, potent inhibitors of Ca^{2+} uptake into the mitochondrial matrix. These results were obtained with diverse respiratory substrates, including glutamate (42, 48), pyruvate (38, 42), and α-ketoglutarate (38), strongly indicating that stimulation of mitochondrial metabolism requires increased matrix [Ca^{2+}]. This conclusion is fully consistent with the known mechanism for stimulation of PDH, which is inactive until dephosphorylated by Ca^{2+}-dependent phosphatases inside the matrix. Perhaps the strongest evidence for Ca^{2+} regulatory sites on the external (OM-facing) surface of the inner membrane has been provided by studies of metabolite carriers. These include the aspartate-glutamate carrier (AGC) and an ATP-Mg^{2+}/P_i exchanger, both of which have been suggested to become stimulated by added Ca^{2+} in the absence of matrix Ca^{2+} uptake (49, 50). AGC has two isoforms (aralar and citrin) with different kinetic characteristics and tissue-specific expression, and both contain N-terminal extensions with Ca^{2+}-binding EF-hand domains accessible in the IMS (50, 51). As this carrier is a key component of the malate-aspartate shuttle (MAS), significantly increasing its activity could be expected to increase substrate uptake and thus support increased ATP production. However, unlike PDH, AGC displays considerable activity in the absence of Ca^{2+}, with only a fractional increase induced by Ca^{2+} in the case of aralar, the predominant isoform in muscle (a 1.5-fold increase in activity with $K_{0.5}$ ∼300 nM) (51). Moreover, the stimulation of MAS activity by external Ca^{2+} is blunted in the absence of Ruthenium Red for reasons that are not yet clear (51). It is possible that an incremental upregulation of MAS elicited by cytosolic Ca^{2+} might complement the stimulation of dehydrogenases by matrix Ca^{2+}, as recently suggested by Rutter et al. (52). However, it seems likely that the Ca^{2+} sensitivity of these carriers is more relevant to tissue-specific stress responses, such as those elicited by glutamate spikes in neuronal cells (53), than to general regulation of mitochondrial ATP production.

4. MITOCHONDRIAL CALCIUM SIGNALING

4.1. Heart

Cardiac ventricular myocytes are ideal for studying Ca^{2+} flux across the IMM, which plays a key role in regulating mitochondrial functions. In the mammalian heart, mitochondria are the primary source of ATP and are more densely packed per unit volume than in any other tissue,

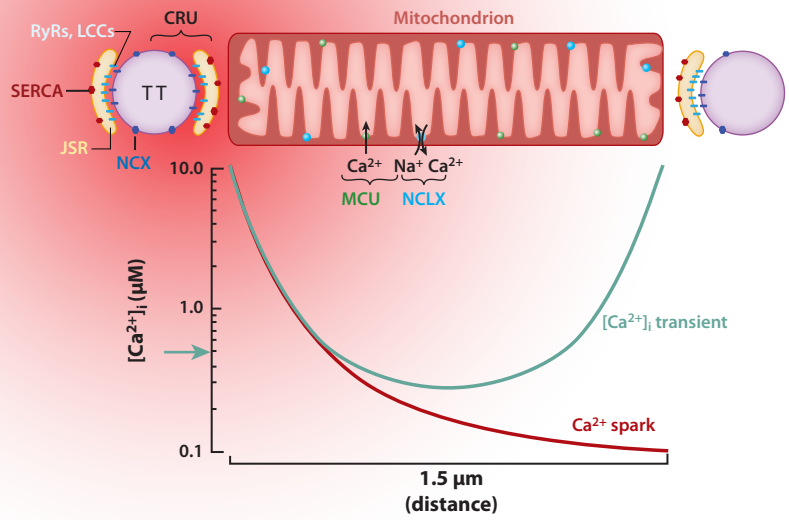

Figure 2

Spatial distribution of cardiac mitochondrial Ca^{2+} signaling components. A spatial representation of a Ca^{2+} spark (*red background gradient*) initiated at the CRU, which is located between the TT and the junctional sarcoplasmic reticulum membranes. At the peak of a Ca^{2+} spark, $[Ca^{2+}]_i$ briefly (10 ms) bathes the end of a mitochondrion with high $[Ca^{2+}]_i$ (5–10 μM). The arrow on the *y*-axis indicates cell-wide (global) peak $[Ca^{+2}]_i$ transient. During a $[Ca^{2+}]_i$ transient, multiple CRUs release Ca^{2+}, bathing both ends of the mitochondrion with high $[Ca^{2+}]_i$. Abbreviations: CRU, Ca^{2+} release unit; LCCs, L-type Ca^{2+} channels; MCU, mitochondrial calcium uniporter; NCLX, mitochondrial sodium calcium exchanger; NCX, sodium calcium exchanger; RyRs, ryanodine receptor type 2; SERCA, sarcoplasmic/endoplasmic reticulum calcium-ATPase; TT, transverse tubule. Figure adapted with permission from Reference 56; copyright 2013 National Academy of Sciences.

constituting roughly one-third of the cell volume. These mitochondria experience regular and repetitive increases in extramitochondrial Ca^{2+} levels, specifically local elevations in cytosolic calcium concentration ($[Ca^{2+}]_i$). The abundant intermyofibrillar mitochondria are situated in close proximity to the sarcoplasmic reticulum (SR), the primary intracellular Ca^{2+} storage organelle, which releases Ca^{2+} with each heartbeat (**Figure 2**). While the cell-averaged (global) $[Ca^{2+}]_i$ increases from 100 nM to ~500 nM during each heartbeat, the localized $[Ca^{2+}]_i$ near

the ends of the intermyofibrillar mitochondria may briefly spike to ∼10 μM during the release phase nearest to the SR Ca^{2+} release units (56, 57). The Ca^{2+} released from the SR can traverse the IMM through the MCU complex, the only established pathway for Ca^{2+} entry into the mitochondrial matrix (58–60). This Ca^{2+} entry is driven by the voltage gradient across the IMM, the mitochondrial membrane potential ($\Delta\Psi_m$), creating a significant negative voltage on the matrix side (ranging from −120 to −160 mV). Ca^{2+} is extruded from the matrix by the mitochondrial Na^+/Ca^{2+} exchanger (NCLX) (61–63), with additional Ca^{2+} efflux via Na^+-independent mechanisms, potentially via a putative transporter termed TMBIM5 (64, 65).

The movement of Ca^{2+} in and out of the mitochondria is very modest compared to the substantial fluxes across the membrane or the SR (56). As a result, normal physiological mitochondrial Ca^{2+} movements do not significantly affect cytosolic $[Ca^{2+}]_i$ levels, and heart mitochondria do not act as a significant dynamic buffer for $[Ca^{2+}]_i$ (45, 56, 66, 67). Nevertheless, these modest mitochondrial Ca^{2+} movements are essential for the physiological regulation of cardiac mitochondrial ATP production. Under physiological conditions, $[Ca^{2+}]_m$ tracks cytosolic $[Ca^{2+}]_i$, but it changes at a much slower rate, acting as a low-pass filter version of the $[Ca^{2+}]_i$. In this manner, the sharp, transient rise of cytosolic $[Ca^{2+}]_i$ with each heartbeat does not produce synchronized, large transients of $[Ca^{2+}]_m$ (42, 68–71). Instead, a series of cytosolic Ca^{2+} transients and their pattern cause a gradual, heart rate–dependent variation in $[Ca^{2+}]_m$, ensuring that mitochondrial ATP production is in sync with changes in heart rate.

4.2. Nonexcitable Cells

In most nonexcitable cells, the endoplasmic reticulum (ER) serves as the primary Ca^{2+} storage organelle, a structure analogous to muscle's SR. The ER houses inositol 1,4,5-trisphosphate receptors (IP_3Rs), which facilitate the release of Ca^{2+} into the cytosol, resulting in cell-wide oscillations or prolonged global elevations of cytosolic Ca^{2+} levels ($[Ca^{2+}]_i$). The activation of IP_3Rs is triggered by both Ca^{2+} and IP_3. The latter is produced enzymatically in response to the stimulation of a variety of plasma membrane receptors by hormones, neurotransmitters, and other extracellular agonists (72–74).

Much of the Ca^{2+} released from ER stores through IP_3Rs diffuses away from the release sites into the cytosol, where it produces global elevations in $[Ca^{2+}]_i$ of only a few hundred nanomolars. Because transport of Ca^{2+} via the uniporter is very slow at submicromolar $[Ca^{2+}]_i$ (see Section 4), mitochondria were generally considered nonresponsive to typical cytosolic Ca^{2+} signals. However, this view was changed in the late 1990s by Rizzuto and colleagues (75) in experiments on living cells expressing targeted Ca^{2+}-sensitive fluorescence probes. The resulting images demonstrated that mitochondria in close proximity to the ER in nonexcitable cells, like those proximal to SR calcium release sites in muscle, are exposed to locally elevated Ca^{2+} levels that can support rapid Ca^{2+} transport into the matrix (75) (for a review, see 76). Such Ca^{2+} microdomains might arise spontaneously and transiently as a natural consequence of organelle crowding in many cell types (as noted in 77). However, there is growing evidence for a level of organization in nonexcitable cells analogous to that in muscle, i.e., specialized interfaces between membranes of the ER and the OMM, possibly stabilized by protein tethers (78, 79). These interfaces are proposed to be involved in a wide range of processes including, but not limited to, Ca^{2+} transport, lipid transfer, and organelle biogenesis and dynamics (79–83). The regions of close association between ER and the mitochondrial surface were referred to as mitochondria-associated membranes (MAMs; 81) in the 1990s and later by a variety of acronyms such as MERCs (84) (mitochondria-ER contacts), and can involve a third cell component, such as lipid droplets (85) or plasma membrane (83). Extended densities observed in electron tomograms to span ER and mitochondria vary in length

(9–30 nm), suggesting the occurrence of multiple types of bridging complexes (79). Subsequently, numerous combinations of ER and mitochondrial OMM proteins have been implicated in forming diverse, function-specific intermembrane complexes (76). Several of the proposed complexes are anchored at the ER by IP_3Rs and at the OMM by the VDAC pore, consistent with involvement in mitochondrial Ca^{2+} uptake from ER stores. In fact, multiple knockouts of IP_3R and VDAC isoforms indicate that these two proteins are essential to the process (86). Modulating the distance between the apposed ER and OMM surfaces by overexpression of synthetic tethers suggests an optimum spanning distance of around 20 nm for mitochondrial Ca^{2+} uptake, influenced by such factors as ion diffusion and steric hindrance of components such as IP_3Rs (79, 84, 86, 87). However, while varying the interface width influences on mitochondrial Ca^{2+} uptake and respiratory parameters, there was no impact on $\Delta\Psi_m$, the inner membrane electrical potential that drives ATP synthesis (86). Also, findings with overexpressed synthetic tethers are complicated by concurrent increases in the extent of OMM and ER surfaces involved in forming the interfaces (79, 84). Thus, considerable work remains to understand how ER-mitochondria and other cellular tethered microdomains, described variously as adaptable and metastable (88, 89), are organized and function within a dynamic cytoplasm. An important step would be determining the molecular components of the ER-OMM bridging densities, e.g., by fitting atomic structures of candidate proteins to high-resolution tether densities obtained by cryogenic electron microscopy (cryo-EM), as done for the attachment of sperm mitochondria to the cytoskeleton via VDAC and glycerol kinase on the OMM (90).

5. THE MCU CHANNEL

Originally described as a mitochondrial calcium uniporter in the 1980s, abbreviated as MCU, nearly 20 years later it was discovered through electrophysiological studies to be a highly selective Ca^{2+} channel (91). Some seven years following this discovery, the first molecular components of the channel were identified (59, 60). These breakthroughs paved the way for the identification of the complete ensemble of subunits that form the channel's holo-complex, known as MCUcx.

5.1. Biophysical Characteristics of the MCU Channel Holo-Complex

Electrophysiological studies by Kirichok and colleagues (91, 92) conclusively demonstrated that the MCUcx is a highly selective, low-conductance Ca^{2+} channel. The channel's single-channel conductance (g_{mcu}) follows a Michaelis-Menten model, with a K_m for $[Ca^{2+}]_i$ of 19 mM. This is significantly higher than the physiological diastolic levels of $[Ca^{2+}]_i$ in the heart, which range from 100 nM to 500 nM. The maximum conductance of MCUcx reaches about 6–7 pS at 105 mM $[Ca^{2+}]_i$ (see 56, 60), which is roughly 10,000 times greater than what is observed under physiological conditions. This relationship between the Ca^{2+} conductance of MCUcx and Ca^{2+} concentration is a common characteristic of highly selective ion channels (93). Typically, the conductance of an open channel increases as the availability of the conducting ion increase (93). Due to these biophysical features, conducting electrophysiological examinations of the MCUcx at physiological $[Ca^{2+}]_i$ levels is particularly challenging. Under these conditions, the single-channel conductance is low, approximately 0.1 fS at 500 nM $[Ca^{2+}]_i$ and a $\Delta\Psi_m$ of −160 mV (see 56). Another limitation to Ca^{2+} flux is the relatively low abundance of MCUcx channels in the IMM membrane of various tissues, including the heart. Consequently, no electrophysiological studies of MCUcx current have been conducted within the $[Ca^{2+}]_i$ range of 300 nM to 10 μM, a range of particular interest where $[Ca^{2+}]_i$-dependent allosteric gating of the MCUcx is proposed to occur (94–102).

The $\Delta\Psi_m$ not only drives Ca^{2+} movement through the MCUcx but it also tightly regulates the stochastic opening and closing of the channel (58, 91, 92). At a $\Delta\Psi_m$ of −80 mV, the open probability is only 0.11 but sharply increases to 0.93 at a $\Delta\Psi_m$ of −160 mV. The structural basis of this voltage-dependent gating remains largely unclear. It is evident, however, that voltage-dependent stochastic opening and closing of the channel persist even in the absence of its auxiliary subunits, such as mitochondrial calcium uptake 1 (MICU1). In this case, the open probability of the MCUcx is two-to-threefold lower than in the wild-type MCUcx that contains MICU1. These findings emphasize the importance of the pore-forming subunits as critical components of the gate and highlight the role of auxiliary subunits as modifiers.

5.2. Molecular Structure and Regulation of MCUcx

The unique subunits that collectively form the MCUcx include EMRE, MCUR1 (mitochondrial calcium uniporter regulator 1), MCUb (mitochondrial calcium uniporter dominant-negative beta subunit), MICUx (comprising mitochondrial calcium uptake 1–3, i.e., MICU1, MICU2, and MICU3), and the pore-forming subunit itself (often referred to simply as MCU), as illustrated in **Figure 3*a***. Understanding the properties and functions of these MCUcx subunits is a challenging and actively evolving area of research.

The Ca^{2+} conduction pathway of the MCUcx consists of four pore-forming subunits (103) (i.e., MCU). Within this tetrameric assembly, the MCU subunits can be substituted with dominant-negative subunits, known as MCUb, which results in a pore with reduced activity (104). MCUb is not as ubiquitous as MCU and is found in fewer tissues (104). Its expression is also thought to be associated with the progression of certain pathological conditions where it is suggested to function as a mechanism to limit mitochondrial Ca^{2+} influx (101, 105–107).

EMRE is a 10-kDa protein with a single transmembrane domain that structurally supports the tetrameric MCU pore (103). In its absence, no channel activity occurs (58, 108, 109). Apart from its pore scaffolding role, EMRE also connects the pore structure with its regulatory subunits MICU1 and MICU2 (103).

Among the three currently known MICUs, MICU1 was the first to be identified (110). Initially, it was thought to be an essential subunit without which the channel could not function (110). However, it later became abundantly evident that MICU1 is not a critical component of the functional channel but rather an auxiliary subunit that regulates its function (58, 99, 108, 109). MICU1 was shown to interact with the MCU pore in the IMS, where it senses Ca^{2+} via EF-hand domains with an apparent Ca^{2+} dissociation constant (K_d) of ∼300 nM for MICU1 (111) and ∼650 nM for MICU2 (111) (not determined quantitatively for MICU3). MICU1 appears to be expressed in every tissue tested (96), and mice lacking MICU1 are either partially (102) or completely (112) perinatal lethal. In contrast, MICU2 and MICU3 are expressed in fewer tissues (113, 114), and mice deficient in MICU2 are viable but develop heart pathology (115). Studying how the MICUs regulate the MCUcx is an area of research that continues to be highly active and rapidly evolving. The current understanding and proposed mechanisms are discussed in more detail in Section 5.3 below.

As our understanding of MCUcx continues to evolve, it becomes clearer that MCU complexes differ significantly across various tissues. The density of MCUcx channels within the IMM varies greatly among mammalian tissues, with the heart exhibiting the lowest levels and skeletal muscle showing the highest among studied tissues. Similarly, there are notable tissue-based differences in the regulation of the open probability of the MCUcx (42, 116), as well as in the stoichiometry of MCU:MCU1:MICU2 in the active channel (117). An additional layer of complexity is introduced through epigenetic regulation by multiple microRNAs (miRNAs). The currently identified range

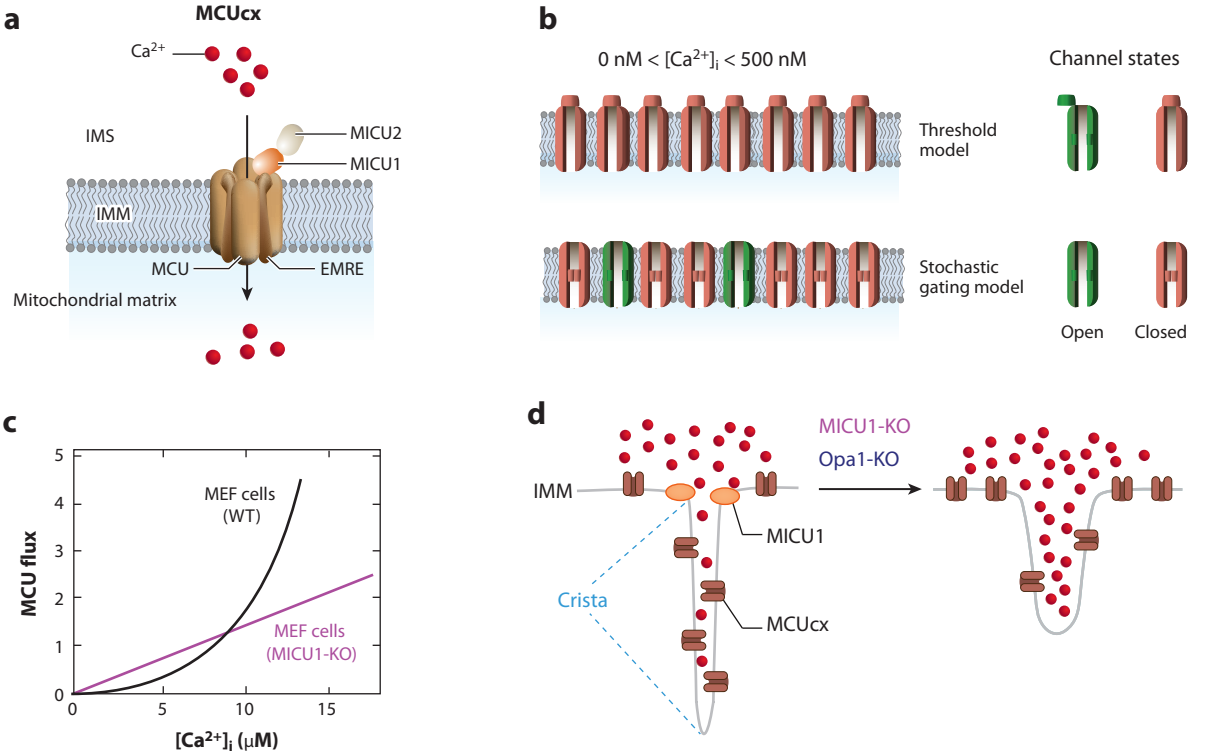

Figure 3

The MCU channel complex and its regulation. (*a*) The molecular components of the MCUcx. (*b*) The two models of MCUcx channel activity at or below threshold $[Ca^{2+}]_i$ (0 to ~500 nM), threshold, and stochastic gating models. (*c*) Representation of typical MCU Ca^{2+} flux from nonexcitable cells, e.g., Reference 58. (*d*) A spatial representation of the structural coupling of MCU function to its mitochondrial location.(*Left*) The Ca^{2+} signaling environment of MCUcx within the IMM when the cristae extend and (*right*) when the crista widens. Abbreviations: EMRE, essential MCU regulatory element; IMM, inner mitochondrial membrane; IMS, intermembrane space; KO, knockout; MCUcx, MCU channel holo-complex; MEF, murine embryonic fibroblast; MICU1/2, mitochondrial calcium uptake 1/2; Opa1, optic atrophy 1; WT, wild-type.

of miRNAs target specific subunits of the channel, each associated with different pathological conditions. For instance, miR-1 downregulates MCU during cardiac hypertrophy (118), miR-25 in aggressive colon cancer cells (119), miR-138 in rapidly proliferating smooth muscle cells (120), and miR-340 in breast cancer cells (121). In parallel, miR-195 has been shown to downregulate MICU1 in ovarian cancer cells (122), and miR-181c plays a role in downregulating MICU1 in the heart as part of the postischemic response (123).

5.3. Multiscale Regulation of MCUcx

Prior to the molecular identification of the proteins that comprise the MCUcx, it was not possible to dissect how each of the various components influences the channel's biophysical characteristics. These include the effects of Ca^{2+} binding to putative regulatory domains of the channel, known since the early 1980s to modulate uniporter behavior by an apparent allosteric mechanism (124, 125). With the discovery of the channel subunits, it became possible to genetically manipulate and alter these proteins, albeit largely in nonexcitable cells (58, 94, 99, 108, 109, 126). Of these subunits, MICU1 had features that drew particular attention. First, its genetic deletion

($MICU1^{-/-}$) significantly affected how the channel functions. Secondly, such deletion was partially (102) or completely (112) embryonic lethal in mice, while deletion of the channel pore-forming units ($MCU^{-/-}$) did not appear to be (127, 128).

As the work evolved, several laboratories reported similar findings, typified by those shown in **Figure 3*c*** for altered expression of MICU1 in multiple cell lines (58). Calcium uptake by the mitochondria of the wild-type cells has a hyperbolic dependence on external [Ca^{2+}], with an apparent $[Ca^{2+}]_i$ threshold well above the resting cytosolic levels. Below this threshold no net flux is measured. Knockout of MICU1, however, removes this threshold and results in a linear dependence of calcium transport on external [Ca^{2+}] through the range 0–15 μM (**Figure 3*c***). The initial hypothesis forwarded to explain this change in channel behavior was a physical steric blockade of the MCU pore by MICU1, which serves as a gatekeeper removed by Ca^{2+} binding (103) (see the top of **Figure 3*b***). Cryo-EM structures of the MCUcx are considered to support such a two-state model by showing MICU1 binding at the MCU pore opening, "sealing" the channel or producing inhibited state (with EGTA, no added Ca^{2+}), but not in an activated state (with 2 mM Ca^{2+}) (103). While these structures provide valuable information about the holo-complex, they do not directly correlate structural differences with the physiological range of [Ca^{2+}] effects. More generally, while a two-state occlusion mechanism might account for a shift from $[Ca^{2+}]_i$ threshold to no threshold in the absence of MICU1, it does not explain why Ca^{2+} transport rates of wild-type mitochondria exceed those of $MICU1^{-/-}$ mitochondria above the $[Ca^{2+}]_i$ threshold. That effect requires a Ca^{2+}-induced change in MCUcx that increases the channel's flux and is reduced or absent without MICU1. In fact, such a mechanism is provided by the calcium dependence of the channel's opening and closing (58). While the open probability of MCUcx is increased 2–3 fold by Ca^{2+} binding to MICU1, the single channel openings occur (albeit at reduced frequency) in the absence of MICU1. This provides a mechanism for potentiation of the channel's current via a stochastic gating model (**Figure 3*b***). Along these lines, it is worth noting that these electrophysiological studies did not find evidence that the channel can become occluded (58). Consequently, it has been proposed (58, 129) that the apparent threshold at low $[Ca^{2+}]_i$ is caused by an as-yet unresolved indirect mechanism that may or may not involve Ca^{2+}-dependent conformational changes within the MCU channel complex itself.

An alternative mechanism for attenuation of mitochondrial Ca^{2+} uptake at low cytosolic Ca^{2+} levels is based on recent evidence that MICU1 is involved in another fundamental mitochondrial process, the folding of the IMM to form cristae. Cristae extend from the peripheral region of the IMM that parallels the OMM, referred to as the inner boundary membrane (IBM), at so-called crista junctions (CJs) (130) that are formed by a multiprotein mitochondrial contact site and cristae organizing system (MICOS) (131, 132). There is evidence that MICU1 binds to the MICOS complex independently of its binding to MCU (133) and that reducing its expression has the same effect of destabilizing cristae (widening CJs and reducing crista surface) as that of Opa1 (133, 134), considered the crista gatekeeper responsive to cellular stresses (135–137). Further, evidence from superresolution microscopy suggests that MICU1 resides exclusively on the IBM while MCU distributes randomly on the IMM (134, 138). These observations suggest a structural coupling of MCU function to its mitochondrial location. The MCU in the IBM sense [Ca^{2+}] in the IMS, at or near the cytosolic level on the other side of the permeable OM. The rest of the MCU channels are located inside cristae where [Ca^{2+}] is normally depleted (134), likely due to restricted diffusion through tight CJs.

By this structural coupling hypothesis (**Figure 3*d***), knockout of MICU1 increases rates of mitochondrial Ca^{2+} uptake at low $[Ca^{2+}]_i$ by widening CJs and reducing crista surface, thereby reducing Ca^{2+} depletion inside crista lumens and increasing the fraction of MCU actively transporting Ca^{2+}. Consistent with this hypothesis, knockout of Opa1 similarly alters crista

structure (as noted above; see also 139) and increases mitochondrial calcium uptake in a variety of cell types, including murine embryonic fibroblast (MEF) cells (140), neurons (141) and liver (142). The increased Ca^{2+} uptake in MEF cells could be attributed in part to closer association of the OMM with proximal ER. However, the evidence that both the stress sensor, Opa1, and Ca^{2+} sensor, MICU1, interact directly with MICOS and possibly MCU at CJs (133, 134) suggests a coupling between mitochondrial Ca^{2+} uptake and IMM topology that remains to be elucidated.

It has long been known that moderate uptake of Ca^{2+} by respiring mitochondria is accompanied by reversible matrix swelling (143). The associated partial unfolding of cristae and possible relocation of MCU, such as that inferred for loss of MICU1 and Opa1 (**Figure 3*d***), could account at least in part for the cooperative nature of Ca^{2+} uptake (**Figure 3*c***). How mitochondria adapt structurally to Ca^{2+} uptake of varying rate and extent, including their capacity to buffer matrix Ca^{2+} [e.g., by sequestration in amorphous calcium phosphate granules (144–146)], is another line of investigation that is reemerging in parallel with advances in technology, e.g., in cryo-EM and superresolution imaging.

6. SIGNALING SYSTEMS THAT COMPLEMENT CALCIUM SIGNALING

The possible function of complementary signaling systems in the heart would address a long-standing metabolic conundrum for heart function: How does consumption of energy contribute to the feedback control of ATP production by mitochondria? The Ca^{2+} feedback mechanism is clearly important because it links mitochondrial ATP production to heart rate by raising $[Ca^{2+}]_m$ levels (42, 68–71), which in turn stimulates processes upstream of the respiratory chain. However, the robust Ca^{2+}-dependent metabolic feedback mechanism alone does not wholly explain how mitochondrial ATP production matches the full range of energy demands in ventricular cardiomyocytes. In particular, it does not provide a signaling process by which elevated cardiac pressure-volume work stimulates concurrent changes in mitochondrial ATP production. This kind of situation arises routinely when the heart must pump at the same rate but against a greater afterload. This occurs, for example, when blood pressure rises.

The regulation of mitochondrial ATP output by systems complementary to that dependent on $[Ca^{2+}]_m$ has been the focus of several investigations in nonexcitable cells (147, 148). These studies raised the possibility that such signaling systems could sense CO_2 generated as a waste product of nutrient oxidation in the mitochondrial matrix. The faster the flux through the Krebs cycle, the greater the carbon emissions. Although CO_2 is a lipid soluble gas that swiftly permeates membranes, a fraction is retained inside mitochondria as bicarbonate, produced by the reaction catalyzed by carbonic anhydrase. Bicarbonate directly activates soluble adenylyl cyclases (sACs), which in turn produce cAMP. Thus, if a sAC is localized in mitochondrial subcompartments, it could monitor local levels of CO_2 (reflecting workload) and, in principle, modulate metabolic output accordingly. Most recently, Greiser et al. (149) showed that a sAC is located within the mitochondria of ventricular myocytes, where it produces cAMP when activated by bicarbonate. They further demonstrated that this cAMP regulates mitochondrial ATP production through a signaling cascade within the IMS, involving sequential activation of exchange protein directly activated by cAMP (EPAC1) and Rap1 (Ras-related protein-1). The results indicate that this workload (CO_2)-dependent cAMP signal activates mitochondrial ATP production machinery independently of, yet synergistically with, the heart-rate dependent $[Ca^{2+}]_m$ signal. The clear implication is that the two signaling pathways operate together to match mitochondrial ATP production to the full range of energy demand in the heart.

The process by which the cAMP signal in the IMS is transmitted to the ATP production machinery is not yet defined and is currently under investigation. Likewise, the existence of two

signaling pathways in heart mitochondria raises important questions about how the different signals are integrated normally and how alterations in each pathway might contribute to both the progression of heart disease and the heart's response to therapeutic interventions.

7. CONCLUDING REMARKS

This review has focused on the elements of calcium regulation of mitochondria related to one function, ATP generation. While parallel research in the last two decades has greatly expanded our understanding of mitochondrial involvement in numerous other fundamental processes (146, 150), ATP production remains the defining characteristic of the powerhouse of the cell. Clearly, understanding the variations in mitochondrial ATP production and its sensitivity to calcium signals across different tissues and cell types remains a crucial goal of future research. An equally important objective is to elucidate the role played by alterations in calcium signaling and in $[Ca^{2+}]_m$-dependent steps of ATP production in the pathogenesis of various diseases. Indeed, mitochondrial dysfunction associated with $[Ca^{2+}]_m$ regulation has been implicated in the etiology of numerous degenerative and age-related diseases (as reviewed in 151, 152). Just as advances in technology have been crucial for understanding organelle cross talk in the cytoplasm and intramitochondrial calcium targets, delineation of specific mechanisms underlying mitochondrial dysfunction in chronic disease will be driven by rapidly accelerating advances in technology, both computational and experimental (e.g., 153). There is little doubt that the ensuing progress will be punctuated by surprises along with a deeper appreciation of the role of calcium in regulating the cell's energy supply.

DISCLOSURE STATEMENT

The authors are not aware of any affiliations, memberships, funding, or financial holdings that might be perceived as affecting the objectivity of this review.

ACKNOWLEDGMENTS

This work was supported by British Heart Foundation grants FS/IBSRF/24/25202 (to L.B.) and PG/21/10661 (to P.S.).

LITERATURE CITED

1. Clapham DE. 2007. Calcium signaling. *Cell* 131:1047–58
2. Cheng H, Lederer WJ. 2008. Calcium sparks. *Physiol. Rev.* 88:1491–545
3. Denton RM, Randle PJ, Martin BR. 1972. Stimulation by calcium ions of pyruvate dehydrogenase phosphate phosphatase. *Biochem. J.* 128:161–63
4. Weibel ER, Staubli W, Gnagi HR, Hess FA. 1969. Correlated morphometric and biochemical studies on the liver cell. I. Morphometric model, stereologic methods, and normal morphometric data for rat liver. *J. Cell Biol.* 42:68–91
5. Veltri KL, Espiritu M, Singh G. 1990. Distinct genomic copy number in mitochondria of different mammalian organs. *J. Cell. Physiol.* 143:160–64
6. Blouin A, Bolender RP, Weibel ER. 1977. Distribution of organelles and membranes between hepatocytes and nonhepatocytes in the rat liver parenchyma. A stereological study. *J. Cell Biol.* 72:441–55
7. Barth E, Stammler G, Speiser B, Schaper J. 1992. Ultrastructural quantitation of mitochondria and myofilaments in cardiac muscle from 10 different animal species including man. *J. Mol. Cell. Cardiol.* 24:669–81
8. van Dyke RW, Gollan JL, Scharschmidt BF. 1983. Oxygen consumption by rat liver: effects of taurocholate and sulfobromophthalein transport, glucagon, and cation substitution. *Am. J. Physiol.* 244:G523–31

9. Bracht L, Caparroz-Assef SM, Bracht A, Bersani-Amado CA. 2016. Effect of the combination of ezetimibe and simvastatin on gluconeogenesis and oxygen consumption in the rat liver. *Basic Clin. Pharmacol. Toxicol.* 118:415–20
10. Shadrin KV, Morgulis II, Pahomova VG, Rupenko AP, Khlebopros RG. 2015. Characteristics of oxygen transport through the surface of the isolated perfused rat liver. *Doklady Biochem. Biophys.* 464:298–300
11. do Nascimento GS, Constantin RP, Gilglioni EH, de Castro Ghizoni CV, Bracht A, et al. 2018. The acute effects of citrus flavanones on the metabolism of glycogen and monosaccharides in the isolated perfused rat liver. *Toxicol. Lett.* 291:158–72
12. de Medeiros HC, Constantin J, Ishii-Iwamoto EL, Mingatto FE. 2015. Effect of fipronil on energy metabolism in the perfused rat liver. *Toxicol. Lett.* 236:34–42
13. Colturato CP, Constantin RP, Maeda AS Jr., Constantin RP, Yamamoto NS, et al. 2012. Metabolic effects of silibinin in the rat liver. *Chem. Biol. Interact.* 195:119–32
14. Cohen JJ, Merkens LS, Peterson OW. 1980. Relation of Na^+ reabsorption to utilization of O_2 and lactate in the perfused rat kidney. *Am. J. Physiol.* 238:F415–27
15. Silva P, Hallac R, Spokes K, Epstein FH. 1982. Relationship among gluconeogenesis, QO_2, and Na^+ transport in the perfused rat kidney. *Am. J. Physiol.* 242:F508–13
16. From AH, Petein MA, Michurski SP, Zimmer SD, Ugurbil K. 1986. ^{31}P-NMR studies of respiratory regulation in the intact myocardium. *FEBS Lett.* 206:257–61
17. From AH, Zimmer SD, Michurski SP, Mohanakrishnan P, Ulstad VK, et al. 1990. Regulation of the oxidative phosphorylation rate in the intact cell. *Biochemistry* 29:3731–43
18. Katz LA, Swain JA, Portman MA, Balaban RS. 1989. Relation between phosphate metabolites and oxygen consumption of heart in vivo. *Am. J. Physiol.* 256:H265–74
19. Portman MA, Heineman FW, Balaban RS. 1989. Developmental changes in the relation between phosphate metabolites and oxygen consumption in the sheep heart in vivo. *J. Clin. Investig.* 83:456–64
20. Zhang J, Duncker DJ, Xu Y, Zhang Y, Path G, et al. 1995. Transmural bioenergetic responses of normal myocardium to high workstates. *Am. J. Physiol.* 268:H1891–905
21. Elliott AC, Smith GL, Allen DG. 1994. The metabolic consequences of an increase in the frequency of stimulation in isolated ferret hearts. *J. Physiol.* 474:147–59
22. Matthews PM, Bland JL, Gadian DG, Radda GK. 1981. The steady-state rate of ATP synthesis in the perfused rat heart measured by ^{31}P NMR saturation transfer. *Biochem. Biophys. Res. Commun.* 103:1052–59
23. Massie BM, Schwartz GG, Garcia J, Wisneski JA, Weiner MW, Owens T. 1994. Myocardial metabolism during increased work states in the porcine left ventricle in vivo. *Circ. Res.* 74:64–73
24. Schwartz GG, Greyson CR, Wisneski JA, Garcia J, Steinman S. 1994. Relation among regional O_2 consumption, high-energy phosphates, and substrate uptake in porcine right ventricle. *Am. J. Physiol.* 266:H521–30
25. Xu Y, Lu L, Zhu P, Schwartz GG. 1998. β-Adrenergic stimulation induces transient imbalance between myocardial substrate uptake and metabolism in vivo. *Am. J. Physiol.* 275:H2181–90
26. Hoppeler H, Hudlicka O, Uhlmann E. 1987. Relationship between mitochondria and oxygen consumption in isolated cat muscles. *J. Physiol.* 385:661–75
27. Ferrara PJ, Verkerke ARP, Brault JJ, Funai K. 2018. Hypothermia decreases O_2 cost for ex vivo contraction in mouse skeletal muscle. *Med. Sci. Sports Exerc.* 50:2015–23
28. McAllister RM, Ogilvie RW, Terjung RL. 1990. Impact of reduced cytochrome oxidase activity on peak oxygen consumption of muscle. *J. Appl. Physiol. 1985* 69:384–89
29. McAllister RM, Terjung RL. 1990. Acute inhibition of respiratory capacity of muscle reduces peak oxygen consumption. *Am. J. Physiol.* 259:C889–96
30. Longden TA, Lederer WJ. 2024. Electro-metabolic signaling. *J. Gen. Physiol.* 156(2):e202313451
31. Wang Z, Ying Z, Bosy-Westphal A, Zhang J, Schautz B, et al. 2010. Specific metabolic rates of major organs and tissues across adulthood: evaluation by mechanistic model of resting energy expenditure. *Am. J. Clin. Nutr.* 92:1369–77
32. Linn TC, Pettit FH, Reed LJ. 1969. α-Keto acid dehydrogenase complexes, X. Regulation of the activity of the pyruvate dehydrogenase complex from beef kidney mitochondria by phosphorylation and dephosphorylation. *PNAS* 62:234–41

33. Denton RM, Richards DA, Chin JG. 1978. Calcium ions and the regulation of NAD^+-linked isocitrate dehydrogenase from the mitochondria of rat heart and other tissues. *Biochem. J.* 176:899–906
34. McCormack JG, Denton RM. 1981. A comparative study of the regulation of Ca^{2+} of the activities of the 2-oxoglutarate dehydrogenase complex and NAD^+-isocitrate dehydrogenase from a variety of sources. *Biochem. J.* 196:619–24
35. McCormack JG, Denton RM. 1979. The effects of calcium ions and adenine nucleotides on the activity of pig heart 2-oxoglutarate dehydrogenase complex. *Biochem. J.* 180:533–44
36. Rutter GA, Denton RM. 1988. Regulation of NAD^+-linked isocitrate dehydrogenase and 2-oxoglutarate dehydrogenase by Ca^{2+} ions within toluene-permeabilized rat heart mitochondria. Interactions with regulation by adenine nucleotides and NADH/NAD^+ ratios. *Biochem. J.* 252:181–89
37. Rutter GA, Denton RM. 1989. Rapid purification of pig heart NAD^+-isocitrate dehydrogenase. Studies on the regulation of activity by Ca^{2+}, adenine nucleotides, Mg^{2+} and other metal ions. *Biochem. J.* 263:445–52
38. McCormack JG. 1985. Characterization of the effects of Ca^{2+} on the intramitochondrial Ca^{2+}-sensitive enzymes from rat liver and within intact rat liver mitochondria. *Biochem. J.* 231:581–95
39. McCormack JG, Halestrap AP, Denton RM. 1990. Role of calcium ions in regulation of mammalian intramitochondrial metabolism. *Physiol. Rev.* 70:391–425
40. Rutter GA. 1990. Ca^{2+}-binding to citrate cycle dehydrogenases. *Int. J. Biochem.* 22:1081–88
41. Denton RM. 2009. Regulation of mitochondrial dehydrogenases by calcium ions. *Biochim. Biophys. Acta* 1787:1309–16
42. Wescott AP, Kao JPY, Lederer WJ, Boyman L. 2019. Voltage-energized calcium-sensitive ATP production by mitochondria. *Nat. Metab.* 1:975–84
43. Glancy B, Balaban RS. 2012. Role of mitochondrial Ca^{2+} in the regulation of cellular energetics. *Biochemistry* 51:2959–73
44. Rasmussen TP, Wu Y, Joiner ML, Koval OM, Wilson NR, et al. 2015. Inhibition of MCU forces extramitochondrial adaptations governing physiological and pathological stress responses in heart. *PNAS* 112:9129–34
45. Kwong JQ, Huo J, Bround MJ, Boyer JG, Schwanekamp JA, et al. 2018. The mitochondrial calcium uniporter underlies metabolic fuel preference in skeletal muscle. *JCI Insight* 3(22):e121689
46. Altamimi TR, Karwi QG, Uddin GM, Fukushima A, Kwong JQ, et al. 2019. Cardiac-specific deficiency of the mitochondrial calcium uniporter augments fatty acid oxidation and functional reserve. *J. Mol. Cell. Cardiol.* 127:223–31
47. Rosencrans WM, Rajendran M, Bezrukov SM, Rostovtseva TK. 2021. VDAC regulation of mitochondrial calcium flux: from channel biophysics to disease. *Cell Calcium* 94:102356
48. Maack C, Cortassa S, Aon MA, Ganesan AN, Liu T, O'Rourke B. 2006. Elevated cytosolic Na^+ decreases mitochondrial Ca^{2+} uptake during excitation-contraction coupling and impairs energetic adaptation in cardiac myocytes. *Circ. Res.* 99:172–82
49. Palmieri L, Pardo B, Lasorsa FM, del Arco A, Kobayashi K, et al. 2001. Citrin and aralar1 are Ca^{2+}-stimulated aspartate/glutamate transporters in mitochondria. *EMBO J.* 20:5060–69
50. Satrustegui J, Pardo B, Del Arco A. 2007. Mitochondrial transporters as novel targets for intracellular calcium signaling. *Physiol. Rev.* 87:29–67
51. Del Arco A, Contreras L, Pardo B, Satrustegui J. 2016. Calcium regulation of mitochondrial carriers. *Biochim. Biophys. Acta* 1863:2413–21
52. Rutter GA, McCormack JG, Halestrap AP, Denton RM. 2020. The roles of cytosolic and intramitochondrial Ca^{2+} and the mitochondrial Ca^{2+}-uniporter (MCU) in the stimulation of mammalian oxidative phosphorylation. *J. Biol. Chem.* 295:10506
53. Rueda CB, Llorente-Folch I, Traba J, Amigo I, Gonzalez-Sanchez P, et al. 2016. Glutamate excitotoxicity and Ca^{2+}-regulation of respiration: role of the Ca^{2+} activated mitochondrial transporters (CaMCs). *Biochim. Biophys. Acta* 1857:1158–66
54. Portzehl H, Caldwell PC, Rueegg JC. 1964. The dependence of contraction and relaxation of muscle fibres from the crab *Maia squinado* on the internal concentration of free calcium ions. *Biochim. Biophys. Acta* 79:581–91

55. Aogaichi T, Evans J, Gabriel J, Plaut GW. 1980. The effects of calcium and lanthanide ions on the activity of bovine heart nicotinamide adenine dinucleotide-specific isocitrate dehydrogenase. *Arch. Biochem. Biophys.* 204:350–56
56. Williams GS, Boyman L, Chikando AC, Khairallah RJ, Lederer WJ. 2013. Mitochondrial calcium uptake. *PNAS* 110:10479–86
57. Wescott AP, Jafri MS, Lederer WJ, Williams GS. 2016. Ryanodine receptor sensitivity governs the stability and synchrony of local calcium release during cardiac excitation-contraction coupling. *J. Mol. Cell. Cardiol.* 92:82–92
58. Garg V, Suzuki J, Paranjpe I, Unsulangi T, Boyman L, et al. 2021. The mechanism of MICU-dependent gating of the mitochondrial Ca^{2+} uniporter. *eLife* 10:e69312
59. Baughman JM, Perocchi F, Girgis HS, Plovanich M, Belcher-Timme CA, et al. 2011. Integrative genomics identifies MCU as an essential component of the mitochondrial calcium uniporter. *Nature* 476:341–45
60. De Stefani D, Raffaello A, Teardo E, Szabo I, Rizzuto R. 2011. A forty-kilodalton protein of the inner membrane is the mitochondrial calcium uniporter. *Nature* 476:336–40
61. Luongo TS, Lambert JP, Gross P, Nwokedi M, Lombardi AA, et al. 2017. The mitochondrial Na^+/Ca^{2+} exchanger is essential for Ca^{2+} homeostasis and viability. *Nature* 545:93–97
62. Palty R, Silverman WF, Hershfinkel M, Caporale T, Sensi SL, et al. 2010. NCLX is an essential component of mitochondrial Na^+/Ca^{2+} exchange. *PNAS* 107:436–41
63. Boyman L, Williams GS, Khananshvili D, Sekler I, Lederer WJ. 2013. NCLX: the mitochondrial sodium calcium exchanger. *J. Mol. Cell. Cardiol.* 59:205–13
64. Austin S, Mekis R, Mohammed SEM, Scalise M, Wang WA, et al. 2022. TMBIM5 is the Ca^{2+}/H^+ antiporter of mammalian mitochondria. *EMBO Rep.* 23:e54978
65. Patron M, Tarasenko D, Nolte H, Kroczek L, Ghosh M, et al. 2022. Regulation of mitochondrial proteostasis by the proton gradient. *EMBO J.* 41:e110476
66. Boyman L, Chikando AC, Williams GS, Khairallah RJ, Kettlewell S, et al. 2014. Calcium movement in cardiac mitochondria. *Biophys. J.* 107:1289–301
67. Kwong JQ, Lu X, Correll RN, Schwanekamp JA, Vagnozzi RJ, et al. 2015. The mitochondrial calcium uniporter selectively matches metabolic output to acute contractile stress in the heart. *Cell Rep.* 12:15–22
68. Lu X, Ginsburg KS, Kettlewell S, Bossuyt J, Smith GL, Bers DM. 2013. Measuring local gradients of intramitochondrial $[Ca^{2+}]$ in cardiac myocytes during sarcoplasmic reticulum Ca^{2+} release. *Circ. Res.* 112:424–31
69. Hamilton S, Terentyeva R, Martin B, Perger F, Li J, et al. 2020. Increased RyR2 activity is exacerbated by calcium leak-induced mitochondrial ROS. *Basic Res. Cardiol.* 115:38
70. Hamilton S, Terentyeva R, Clements RT, Belevych AE, Terentyev D. 2021. Sarcoplasmic reticulum-mitochondria communication; implications for cardiac arrhythmia. *J. Mol. Cell. Cardiol.* 156:105–13
71. Hamilton S, Terentyeva R, Kim TY, Bronk P, Clements RT, et al. 2018. Pharmacological modulation of mitochondrial Ca^{2+} content regulates sarcoplasmic reticulum Ca^{2+} release via oxidation of the ryanodine receptor by mitochondria-derived reactive oxygen species. *Front. Physiol.* 9:1831
72. Meldolesi J, Pozzan T. 1998. The endoplasmic reticulum Ca^{2+} store: a view from the lumen. *Trends Biochem. Sci* 23:10–14
73. Mak DO, Foskett JK. 2015. Inositol 1,4,5-trisphosphate receptors in the endoplasmic reticulum: a single-channel point of view. *Cell Calcium* 58:67–78
74. Foskett JK, White C, Cheung KH, Mak DO. 2007. Inositol trisphosphate receptor Ca^{2+} release channels. *Physiol. Rev.* 87:593–658
75. Rizzuto R, Pinton P, Carrington W, Fay FS, Fogarty KE, et al. 1998. Close contacts with the endoplasmic reticulum as determinants of mitochondrial Ca^{2+} responses. *Science* 280:1763–66
76. Cartes-Saavedra B, Ghosh A, Hajnoczky G. 2025. The roles of mitochondria in global and local intracellular calcium signalling. *Nat. Rev. Mol. Cell Biol.* 26(6):456–75
77. Boyman L, Karbowski M, Lederer WJ. 2020. Regulation of mitochondrial ATP production: Ca^{2+} signaling and quality control. *Trends Mol. Med.* 26:21–39

78. Boncompagni S, Rossi AE, Micaroni M, Beznoussenko GV, Polishchuk RS, et al. 2009. Mitochondria are linked to calcium stores in striated muscle by developmentally regulated tethering structures. *Mol. Biol. Cell* 20:1058–67
79. Csordas G, Renken C, Varnai P, Walter L, Weaver D, et al. 2006. Structural and functional features and significance of the physical linkage between ER and mitochondria. *J. Cell Biol.* 174:915–21
80. Szabadkai G, Bianchi K, Varnai P, De Stefani D, Wieckowski MR, et al. 2006. Chaperone-mediated coupling of endoplasmic reticulum and mitochondrial Ca^{2+} channels. *J. Cell Biol.* 175:901–11
81. Vance JE. 2014. MAM (mitochondria-associated membranes) in mammalian cells: lipids and beyond. *Biochim. Biophys. Acta* 1841:595–609
82. Lewis SC, Uchiyama LF, Nunnari J. 2016. ER-mitochondria contacts couple mtDNA synthesis with mitochondrial division in human cells. *Science* 353:aaf5549
83. Casler JC, Harper CS, White AJ, Anderson HL, Lackner LL. 2024. Mitochondria-ER-PM contacts regulate mitochondrial division and PI(4)P distribution. *J. Cell Biol.* 223:e202308144
84. Giacomello M, Pellegrini L. 2016. The coming of age of the mitochondria-ER contact: a matter of thickness. *Cell Death Differ*. 23:1417–27
85. Freyre CAC, Rauher PC, Ejsing CS, Klemm RW. 2019. MIGA2 links mitochondria, the ER, and lipid droplets and promotes de novo lipogenesis in adipocytes. *Mol. Cell* 76:811–25.e14
86. Dematteis G, Tapella L, Casali C, Talmon M, Tonelli E, et al. 2024. ER-mitochondria distance is a critical parameter for efficient mitochondrial Ca^{2+} uptake and oxidative metabolism. *Commun. Biol.* 7:1294
87. Csordas G, Varnai P, Golenar T, Roy S, Purkins G, et al. 2010. Imaging interorganelle contacts and local calcium dynamics at the ER-mitochondrial interface. *Mol. Cell* 39:121–32
88. Wu H, Carvalho P, Voeltz GK. 2018. Here, there, and everywhere: the importance of ER membrane contact sites. *Science* 361:eaan5835
89. Obara CJ, Nixon-Abell J, Moore AS, Riccio F, Hoffman DP, et al. 2024. Motion of VAPB molecules reveals ER-mitochondria contact site subdomains. *Nature* 626:169–76
90. Leung MR, Zenezini Chiozzi R, Roelofs MC, Hevler JF, Ravi RT, et al. 2021. In-cell structures of conserved supramolecular protein arrays at the mitochondria-cytoskeleton interface in mammalian sperm. *PNAS* 118:e2110996118
91. Kirichok Y, Krapivinsky G, Clapham DE. 2004. The mitochondrial calcium uniporter is a highly selective ion channel. *Nature* 427:360–64
92. Fieni F, Lee SB, Jan YN, Kirichok Y. 2012. Activity of the mitochondrial calcium uniporter varies greatly between tissues. *Nat. Commun.* 3:1317
93. Hille B. 1992. *Ionic Channels of Excitable Membranes*. Sinauer Associates
94. Csordas G, Golenar T, Seifert EL, Kamer KJ, Sancak Y, et al. 2013. MICU1 controls both the threshold and cooperative activation of the mitochondrial Ca^{2+} uniporter. *Cell Metab*. 17:976–87
95. Patron M, Checchetto V, Raffaello A, Teardo E, Vecellio Reane D, et al. 2014. MICU1 and MICU2 finely tune the mitochondrial Ca^{2+} uniporter by exerting opposite effects on MCU activity. *Mol. Cell* 53:726–37
96. Vecellio Reane D, Vallese F, Checchetto V, Acquasaliente L, Butera G, et al. 2016. A MICU1 splice variant confers high sensitivity to the mitochondrial Ca^{2+} uptake machinery of skeletal muscle. *Mol. Cell* 64:760–73
97. Paillard M, Csordas G, Huang KT, Varnai P, Joseph SK, Hajnoczky G. 2018. MICU1 interacts with the D-ring of the MCU pore to control its Ca^{2+} flux and sensitivity to Ru360. *Mol. Cell* 72:778–85.e3
98. Debattisti V, Horn A, Singh R, Seifert EL, Hogarth MW, et al. 2019. Dysregulation of mitochondrial Ca^{2+} uptake and sarcolemma repair underlie muscle weakness and wasting in patients and mice lacking MICU1. *Cell Rep*. 29:1274–86.e6
99. Mallilankaraman K, Doonan P, Cardenas C, Chandramoorthy HC, Muller M, et al. 2012. MICU1 is an essential gatekeeper for MCU-mediated mitochondrial Ca^{2+} uptake that regulates cell survival. *Cell* 151:630–44
100. Tsai MF, Phillips CB, Ranaghan M, Tsai CW, Wu Y, et al. 2016. Dual functions of a small regulatory subunit in the mitochondrial calcium uniporter complex. *eLife* 5:e15545

101. Lambert JP, Luongo TS, Tomar D, Jadiya P, Gao E, et al. 2019. MCUB regulates the molecular composition of the mitochondrial calcium uniporter channel to limit mitochondrial calcium overload during stress. *Circulation* 140:1720–33
102. Liu JC, Liu J, Holmstrom KM, Menazza S, Parks RJ, et al. 2016. MICU1 serves as a molecular gatekeeper to prevent in vivo mitochondrial calcium overload. *Cell Rep*. 16:1561–73
103. Fan M, Zhang J, Tsai CW, Orlando BJ, Rodriguez M, et al. 2020. Structure and mechanism of the mitochondrial Ca^{2+} uniporter holocomplex. *Nature* 582:129–33
104. Raffaello A, De Stefani D, Sabbadin D, Teardo E, Merli G, et al. 2013. The mitochondrial calcium uniporter is a multimer that can include a dominant-negative pore-forming subunit. *EMBO J.* 32:2362–76
105. Huo J, Lu S, Kwong JQ, Bround MJ, Grimes KM, et al. 2020. MCUb induction protects the heart from postischemic remodeling. *Circ. Res.* 127:379–90
106. Feno S, Munari F, Reane DV, Gissi R, Hoang DH, et al. 2021. The dominant-negative mitochondrial calcium uniporter subunit MCUb drives macrophage polarization during skeletal muscle regeneration. *Sci. Signal* 14:eabf3838
107. Huo J, Prasad V, Grimes KM, Vanhoutte D, Blair NS, et al. 2023. MCUb is an inducible regulator of calcium-dependent mitochondrial metabolism and substrate utilization in muscle. *Cell Rep*. 42:113465
108. Sancak Y, Markhard AL, Kitami T, Kovacs-Bogdan E, Kamer KJ, et al. 2013. EMRE is an essential component of the mitochondrial calcium uniporter complex. *Science* 342:1379–82
109. Kovacs-Bogdan E, Sancak Y, Kamer KJ, Plovanich M, Jambhekar A, et al. 2014. Reconstitution of the mitochondrial calcium uniporter in yeast. *PNAS* 111:8985–90
110. Perocchi F, Gohil VM, Girgis HS, Bao XR, McCombs JE, et al. 2010. MICU1 encodes a mitochondrial EF hand protein required for Ca^{2+} uptake. *Nature* 467:291–96
111. Kamer KJ, Grabarek Z, Mootha VK. 2017. High-affinity cooperative Ca^{2+} binding by MICU1-MICU2 serves as an on-off switch for the uniporter. *EMBO Rep*. 18:1397–411
112. Antony AN, Paillard M, Moffat C, Juskeviciute E, Correnti J, et al. 2016. MICU1 regulation of mitochondrial Ca^{2+} uptake dictates survival and tissue regeneration. *Nat. Commun.* 7:10955
113. Patron M, Granatiero V, Espino J, Rizzuto R, De Stefani D. 2019. MICU3 is a tissue-specific enhancer of mitochondrial calcium uptake. *Cell Death Differ*. 26:179–95
114. Plovanich M, Bogorad RL, Sancak Y, Kamer KJ, Strittmatter L, et al. 2013. MICU2, a paralog of MICU1, resides within the mitochondrial uniporter complex to regulate calcium handling. *PLOS ONE* 8:e55785
115. Bick AG, Wakimoto H, Kamer KJ, Sancak Y, Goldberger O, et al. 2017. Cardiovascular homeostasis dependence on MICU2, a regulatory subunit of the mitochondrial calcium uniporter. *PNAS* 114:E9096–104
116. Boyman L, Greiser M, Lederer WJ. 2021. Calcium influx through the mitochondrial calcium uniporter holocomplex, MCUcx. *J. Mol. Cell. Cardiol.* 151:145–54
117. Paillard M, Csordas G, Szanda G, Golenar T, Debattisti V, et al. 2017. Tissue-specific mitochondrial decoding of cytoplasmic Ca^{2+} signals is controlled by the stoichiometry of MICU1/2 and MCU. *Cell Rep*. 18:2291–300
118. Zaglia T, Ceriotti P, Campo A, Borile G, Armani A, et al. 2017. Content of mitochondrial calcium uniporter (MCU) in cardiomyocytes is regulated by microRNA-1 in physiologic and pathologic hypertrophy. *PNAS* 114:E9006–15
119. Marchi S, Lupini L, Patergnani S, Rimessi A, Missiroli S, et al. 2013. Downregulation of the mitochondrial calcium uniporter by cancer-related miR-25. *Curr. Biol.* 23:58–63
120. Hong Z, Chen KH, DasGupta A, Potus F, Dunham-Snary K, et al. 2017. MicroRNA-138 and microrna-25 down-regulate mitochondrial calcium uniporter, causing the pulmonary arterial hypertension cancer phenotype. *Am. J. Respir. Crit. Care Med.* 195:515–29
121. Yu C, Wang Y, Peng J, Shen Q, Chen M, et al. 2017. Mitochondrial calcium uniporter as a target of microRNA-340 and promoter of metastasis via enhancing the Warburg effect. *Oncotarget* 8:83831–44
122. Rao G, Dwivedi SKD, Zhang Y, Dey A, Shameer K, et al. 2020. MicroRNA-195 controls MICU1 expression and tumor growth in ovarian cancer. *EMBO Rep*. 21:e48483

123. Banavath HN, Roman B, Mackowski N, Biswas D, Afzal J, et al. 2019. miR-181c activates mitochondrial calcium uptake by regulating MICU1 in the heart. *J. Am. Heart Assoc.* 8:e012919
124. Bragadin M, Pozzan T, Azzone GF. 1979. Kinetics of Ca^{2+} carrier in rat liver mitochondria. *Biochemistry* 18:5972–78
125. Kroner H. 1986. "Allosteric regulation" of calcium-uptake in rat liver mitochondria. *Biol. Chem.* 367:483–93
126. Kamer KJ, Mootha VK. 2015. The molecular era of the mitochondrial calcium uniporter. *Nat. Rev. Mol. Cell Biol.* 16:545–53
127. Holmstrom KM, Pan X, Liu JC, Menazza S, Liu J, et al. 2015. Assessment of cardiac function in mice lacking the mitochondrial calcium uniporter. *J. Mol. Cell. Cardiol.* 85:178–82
128. Pan X, Liu J, Nguyen T, Liu C, Sun J, et al. 2013. The physiological role of mitochondrial calcium revealed by mice lacking the mitochondrial calcium uniporter. *Nat. Cell Biol.* 15:1464–72
129. Boyman L, Lederer WJ. 2020. How the mitochondrial calcium uniporter complex (MCUcx) works. *PNAS* 117:22634–36
130. Frey TG, Mannella CA. 2000. The internal structure of mitochondria. *Trends Biochem. Sci.* 25:319–24
131. Harner M, Korner C, Walther D, Mokranjac D, Kaesmacher J, et al. 2011. The mitochondrial contact site complex, a determinant of mitochondrial architecture. *EMBO J.* 30:4356–70
132. Zerbes RM, Bohnert M, Stroud DA, von der Malsburg K, Kram A, et al. 2012. Role of MINOS in mitochondrial membrane architecture: cristae morphology and outer membrane interactions differentially depend on mitofilin domains. *J. Mol. Biol.* 422:183–91
133. Tomar D, Thomas M, Garbincius JF, Kolmetzky DW, Salik O, et al. 2023. MICU1 regulates mitochondrial cristae structure and function independently of the mitochondrial Ca^{2+} uniporter channel. *Sci. Signal.* 16:eabi8948
134. Gottschalk B, Klec C, Leitinger G, Bernhart E, Rost R, et al. 2019. MICU1 controls cristae junction and spatially anchors mitochondrial Ca^{2+} uniporter complex. *Nat. Commun.* 10:3732
135. Frezza C, Cipolat S, Martins de Brito O, Micaroni M, Beznoussenko GV, et al. 2006. OPA1 controls apoptotic cristae remodeling independently from mitochondrial fusion. *Cell* 126:177–89
136. Patten DA, Wong J, Khacho M, Soubannier V, Mailloux RJ, et al. 2014. OPA1-dependent cristae modulation is essential for cellular adaptation to metabolic demand. *EMBO J.* 33:2676–91
137. Gilkerson R, Kaur H, Carrillo O, Ramos I. 2024. OMA1-mediated mitochondrial dynamics balance organellar homeostasis upstream of cellular stress responses. *Int. J. Mol. Sci.* 25:4566
138. Hirtl M, Gottschalk B, Bachkoenig OA, Oflaz FE, Madreiter-Sokolowski C, et al. 2025. A novel super-resolution STED microscopy analysis approach to observe spatial MCU and MICU1 distribution dynamics in cells. *Biochim. Biophys. Acta. Mol. Cell Res.* 1872:119900
139. Fry MY, Navarro PP, Hakim P, Ananda VY, Qin X, et al. 2024. In situ architecture of Opa1-dependent mitochondrial cristae remodeling. *EMBO J.* 43:391–413
140. Cartes-Saavedra B, Macuada J, Lagos D, Arancibia D, Andres ME, et al. 2021. OPA1 modulates mitochondrial Ca^{2+} uptake through ER-mitochondria coupling. *Front. Cell Dev. Biol.* 9:774108
141. Gomez-Valades AG, Pozo M, Varela L, Boudjadja MB, Ramirez S, et al. 2021. Mitochondrial cristae-remodeling protein OPA1 in POMC neurons couples Ca^{2+} homeostasis with adipose tissue lipolysis. *Cell Metab.* 33:1820–35.e9
142. Lee H, Lee TJ, Galloway CA, Zhi W, Xiao W, et al. 2023. The mitochondrial fusion protein OPA1 is dispensable in the liver and its absence induces mitohormesis to protect liver from drug-induced injury. *Nat. Commun.* 14:6721
143. Crofts AR, Chappell JB. 1965. Calcium ion accumulation and volume changes of isolated liver mitochondria. Reversal of calcium ion-induced swelling. *Biochem. J.* 95:387–92
144. Greenawalt JW, Rossi CS, Lehninger AL. 1964. Effect of active accumulation of calcium and phosphate ions on the structure of rat liver mitochondria. *J. Cell Biol.* 23:21–38
145. Wolf SG, Mutsafi Y, Dadosh T, Ilani T, Lansky Z, et al. 2017. 3D visualization of mitochondrial solid-phase calcium stores in whole cells. *eLife* 6:e29929
146. Strubbe-Rivera JO, Chen J, West BA, Parent KN, Wei GW, Bazil JN. 2021. Modeling the effects of calcium overload on mitochondrial ultrastructural remodeling. *Appl. Sci.* 11:2071

147. Acin-Perez R, Salazar E, Kamenetsky M, Buck J, Levin LR, Manfredi G. 2009. Cyclic AMP produced inside mitochondria regulates oxidative phosphorylation. *Cell Metab*. 9:265–76
148. Zippin JH, Chen Y, Nahirney P, Kamenetsky M, Wuttke MS, et al. 2003. Compartmentalization of bicarbonate-sensitive adenylyl cyclase in distinct signaling microdomains. *FASEB J*. 17:82–84
149. Greiser M, Karbowski M, Kaplan AD, Coleman AK, Verhoeven N, et al. 2023. Calcium and bicarbonate signaling pathways have pivotal, resonating roles in matching ATP production to demand. *eLife* 12:e84204
150. Picard M, Shirihai OS. 2022. Mitochondrial signal transduction. *Cell Metab*. 34:1620–53
151. Boyman L, Williams GS, Lederer WJ. 2015. The growing importance of mitochondrial calcium in health and disease. *PNAS* 112:11150–51
152. Boyman L, Karbowski M, Lederer WJ. 2019. Regulation of mitochondrial ATP production: Ca^{2+} signaling and quality control. *Trends Mol. Med.* 26:21–39
153. 2024. Method of the Year 2024: spatial proteomics. *Nat. Methods* 21:2195–96